Study of irradiation temperature effect on change of structural, optical and strength properties of BeO ceramics when irradiated with Ar^{8+} and Xe^{22} heavy ions

A.E. Ryskulov[1], M.V. Zdorovets[1,2,3], A.L. Kozlovskiy[1,2*], D.I. Shlimas[1,2], S.B. Kislitsin[2], Uglov V.V.[4]

[1]*L.N. Gumilyov Eurasian National University, Nur-Sultan, Kazakhstan*
[2]*The Institute of Nuclear Physics of Republic of Kazakhstan, Almaty, Kazakhstan*
[3]*Ural Federal University, Yekaterinburg, Russia*
[4]*Belarusian State University, Minsk, Belarus*
*E-mail: kozlovskiy.a@inp.kz

Abstract
This paper presents the results of the study of the effect of irradiation temperature on structural and optical distortions and deformations, as well as the strength properties of BeO ceramics as a result of irradiation with Ar^{8+} and Xe^{22+} ions at a radiation dose of $5x10^{13}$ cm^{-2}. The choice of radiation dose is due to the effect of overlapping defective areas arising along the trajectories of ions in ceramics, which makes it possible to model radiation damage caused by the effect of accumulation as a result of cascade collisions and overlapping damaged areas. The temperature range of 300-1000 K was chosen to simulate different operating conditions, as well as the possibility of simulating partial annealing of defects during irradiation at high temperatures. During the research it was established that high-temperature radiation reduces influence of size of electronic and nuclear power losses of ions of Ar^{8+} and Xe^{22+} with energy of 70 MeV and 231 MeV, respectively, on extent of radiation damage of ceramics of BeO. Irradiation at a temperature of 1000 K results in an equal 14% change in dislocation density for these particles, a comparable decrease in the yield intensity of optically stimulated luminescence by 5% and 15%, as well as microhardness by 25% and 30%, respectively.
Key words: swift heavy ion, radiation resistance, defects, annealing, nuclear materials

Introduction

На сегодняшний день в современном материаловедении наиболее перспективными материалами, использующимися в различных отраслях науки и техники, являются оксидные наноматериалы или керамики, перовскитные структуры, сегнетоэлектрические и диэлектрические керамики [1-10]. Интерес к ним обусловлен их уникальными физико-химическими свойствами, высокими показателями устойчивости к внешним воздействиям, включающим радиационные повреждения, термический нагрев, агрессивное воздействие кислотных или щелочных сред. В большинстве случаев использование данных типов материалов ограничивается их сроком эксплуатации, которое определяется сохранением показателей устойчивости к внешним воздействиям в течение длительного времени [11-14]. При этом в случае применения данных оксидных наноструктурных керамик или перовскитов в качестве конструкционных материалов наиболее важным условием применимости является их устойчивость к радиационному охрупчиванию и деградации физических и механических свойств [15,16].
One of the main requirements for structural materials for nuclear reactors is to ensure the stability of operating characteristics such as thermal conductivity, electrical resistance, high radiation and corrosion resistance to external influences such as radiation, thermal heating, etc. [17-19]. As is known, the impact of ionizing radiation leads to the accumulation of defects and changes in structural characteristics, the formation of areas of disorder and amorphous inclusions in the near-surface layer, which, in turn, leads to a decrease in thermal conductivity and further

deterioration of the performance characteristics of structural materials [20,21]. Therefore, the research of defect formation processes and the study of radiation resistance of new types of structural materials are of scientific and practical interest. Structural materials based on beryllium or its oxide form have found their application not only as components for optical devices, but also as reflectors and moderators for nuclear reactors [22-24]. Moreover, the use of ceramics of this class can significantly increase the temperature of the working area, which is due to the high values of the melting temperature, thermal conductivity, strength, and also resistance to external influences. However, the use of ceramics based on oxides, carbides or nitrides, which have a similar nature of physicochemical and strength properties, as structural materials for nuclear power in the XXI century requires studying the resistance of these materials to the effects of ionizing radiation, as well as subsequent processes of defect formation [25-30]. At the same time, the service life of these structural materials, approved during the construction of nuclear power plants, must be determined with high accuracy, which is due not only to the strict requirement to minimize the risk of deformation of the vessel structure or the main components of nuclear reactors exposed to radiation, as well as the impossibility of quickly replacing deformed components from - for the accumulated background radiation during operation. The main sources that create defects in structural materials of nuclear reactors during operation are neutron radiation and fragments of fission of uranium nuclei with an energy of 50-250 MeV, which can lead to partial disordering and deformation of the structure as a result of the accumulation effect [31-36]. In this case, the greater the energy of the incident particles, the more defects are created along the trajectory of the ions in the material. Most defects are annihilated during migration, which leads to relaxation of deformations and microstresses. However, at high irradiation densities, defect overlap regions are formed, which form regions with a nonequilibrium defect concentration, which leads to disordering and further amorphization of the structure and a decrease in the ceramic hardness along the entire ion path, as well as to the formation of additional optical traps and an increase in the photoionization cross section affecting the reflection ability of ceramics BeO [37,38]. However, the question still remains open related to the behavior of the structural and strength properties of BeO ceramics to high-temperature irradiation. As is known, when materials are heated, partial annealing and relaxation of defects occurs due to changes in the vibrational modes of atoms and subsequent annihilation of point defects with each other [39-41]. In this case, during the passage of heavy ions in the material, according to the theory of thermal peaks, regions with an increased temperature are formed along the trajectory of the ions, in which defects are formed [42-46]. Moreover, these regions have short lifetimes, but very high temperatures, which leads to the formation of a large number of mobile defects [44-46]. In the case of high-temperature irradiation, the process of defect formation and their annealing will be competing processes, while the question of which of the two processes will dominate in the case when the ion trajectories and, therefore, the defect regions arising from irradiation will overlap at high radiation doses is not clear. In this regard, the study of the processes of radiation damage to ceramics BeO during high-temperature irradiation with high-energy heavy ions is an urgent and demanded direction of scientific research in the field of nuclear technologies.

The main purpose of this work is to conduct research on the effect of the irradiation temperature on the degree of structural distortions and changes in the optical and strength properties of ceramics based on beryllium oxide under irradiation with heavy Ar^{8+} and Xe^{22+} ions. The relevance of this work is due to the acquisition of new experimental data on the processes of radiation damage during irradiation with heavy ions of structural materials based on oxide ceramics, which have broad prospects for use in thermonuclear and nuclear power engineering when creating reactors of the GenIV generation [47-52]. The proposed hypothesis is based on the assumption that, under high-temperature irradiation, some of the point defects will annihilate among themselves due to accelerated vibrations of the atomic lattice not only in the area of damage as a result of local heating during the passage of ions through the material, but also as a result of subsequent cascade collisions. In this case, the supply of heat for heating the sample

during irradiation will significantly increase the amplitude of the vibrational (thermal) motion of the lattice atoms, which will lead to a higher mobility of vacancies and interstitial atoms, with a subsequent decrease in the concentration of point defects during irradiation due to their annihilation.

Experimental part

The objects of study were samples of ceramics based on BeO with a thickness of 15 μm and an area of 5×5 mm. According to the technical data sheet, the chemical purity of beryllium oxide samples was 99.9%. The samples under study were polycrystalline structures with a hexagonal lattice of the space group of symmetry P63mc(186), crystal lattice parameters *a*=2.671 Å, c=4.332 Å (PDF – 01-077-9751). Выбор типа керамик в качестве объекта исследований обусловлен их огромным потенциалом применения в качестве конструкционных материалов для ядерной энергетики нового поколения. В качестве образцов использовались тестовые образцы материалов, которые в дальнейшем планируется использовать в качестве основы для конструкционных материалов высокотемпературных ядерных реакторов.

Irradiation was carried out on DC-60 heavy ion accelerator of the Astana branch of the Institute of Nuclear Physics (Nur-Sultan, Kazakhstan) by Ar^{8+} and Xe^{22+} ions with energies of 70 MeV and 231 MeV, respectively, at irradiation temperatures of 300, 800, 1000 K and a particle fluence of 5×10^{13} cm^{-2}. Облучение исследуемых образцов проводилось в вакууме, образцы помещались на специальные держатели, совмещенные с нагревательным элементом. Контроль температуры проводился с помощью термопар. Контроль дозы облучения проводился с помощью цилиндра Фарадея. Выбор условий облучения и температурного диапазона позволил с высокой точностью смоделировать процессы радиационных повреждений, возникающих в результате деления ядер урана в ядерном реакторе.

Table 1 shows the data on the energy losses of incident ions as a result of interaction with the BeO target, obtained using the simulation method in the SRIM Pro 2013 program code.

Table 1. Energy loss data

Ion energy, MeV	Maximum path length, μm	Deviation, nm	$dE/dx_{electr.}$, keV/μm	$dE/dx_{nucl.}$, keV/μm	Number of vacancies resulting from the interaction of one ion
Ar^{8+}, 70 MeV	11.9±0.5	340±10	6452±150	7.4±0.7	4500±200
Xe^{22+}, 231 MeV	14.5±0.6	412±10	22400±300	56±2.2	29636±300

The Monte Carlo simulation in the SRIM-2013 program of BeO ceramics irradiation at a temperature of 300 K by Ar^{8+} and Xe^{22+} ions with energies of 70 MeV and 231 MeV, respectively, indicates a significant predominance of radiation damage degree during xenon ion irradiation in comparison with argon ion irradiation, which is associated with higher energy losses of xenon ions by approximately three times when interacting with the electronic and nuclear subsystems of the target (See Fig.1).

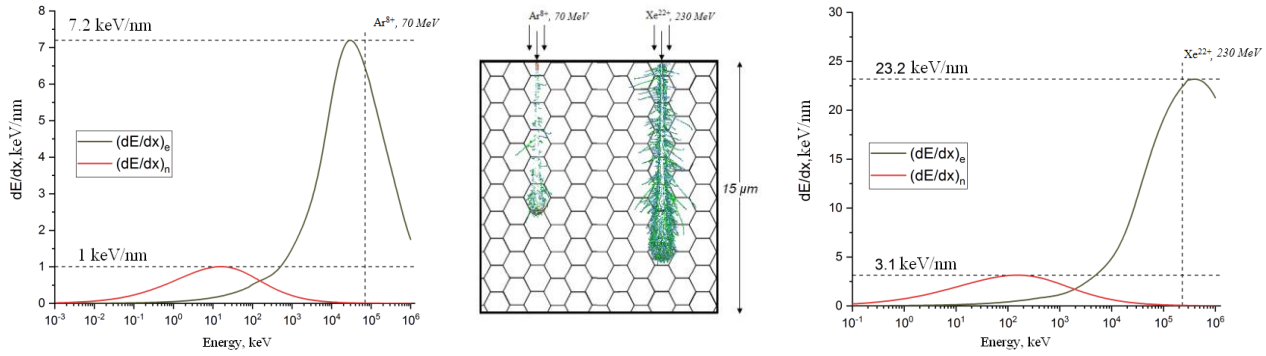

a) b) c)

Figure 1. Calculations in the SRIM-2013 program of electronic $(dE/dx)_e$ and nuclear $(dE/dx)_n$ losses in BeO depending on the energy of Ar^{8+} and Xe^{22+} ions: a) energy losses of Ar^{8+} ions; b) a model of the ion damage cascade in the ceramic structure; c) energy losses of Xe^{22+} ions

According to the calculated data in Table 1, irradiation with Xe^{22+} ions with an energy of 231 MeV is characterized by a greater spatial development of the damage cascade created in the structure of beryllium oxide in comparison with irradiation with Ar^{8+} ions with an energy of 70 MeV, which is caused by about three times higher values of energy losses xenon ions when interacting with the electronic and nuclear subsystems of the material. This is additionally confirmed by the results of calculating the number of vacancies created in the structure, which in the case of irradiation with Xe^{22+} ions is more than six times higher than that for irradiation with Ar^{8+} ions.

The study of changes in structural parameters, including distortions of the crystal lattice and dislocation density, was carried out on the basis of the obtained X-ray diffraction data performed on a D8 ADVANCE ECO powder diffractometer (Bruker, Germany) using CuKα radiation. Съемка дифрактограмм проводилась в геометрии Брегг-Брентано, в угловом диапазоне 2θ=30-75°, с шагом 0.02°, время набора спектра 3 сек в точке. Определение кристаллографических параметров проводилось с помощью программного кода DiffracEVA V.4.2.

Optically stimulated luminescence (OSL) measurements were performed on an automated TL-OSL setup (RNL Denmark). To initiate luminescence, a LED with a wavelength of 470 nm and a power of 35 mW/cm^2 was used. Linear Modulated OSL (LM-OSL) was measured at room temperature after preheating the samples to 160°C at a rate of 5°C/s and holding for 10 s. This procedure is necessary to remove unstable signals.

Determination of microhardness and changes in strength characteristics as a result of irradiation was carried out using the indentation method under variable load, on a digital microhardness meter. The Vickers pyramid was used as an indenter.

Results and discussion

Figure 2a-b show the dynamics of changes in the X-ray diffraction patterns of the studied BeO ceramics irradiated with Ar^{8+} and Xe^{22+} ions at a radiation dose of $5x10^{13}$ cm^{-2} and temperatures of 300, 800, and 1000 K.

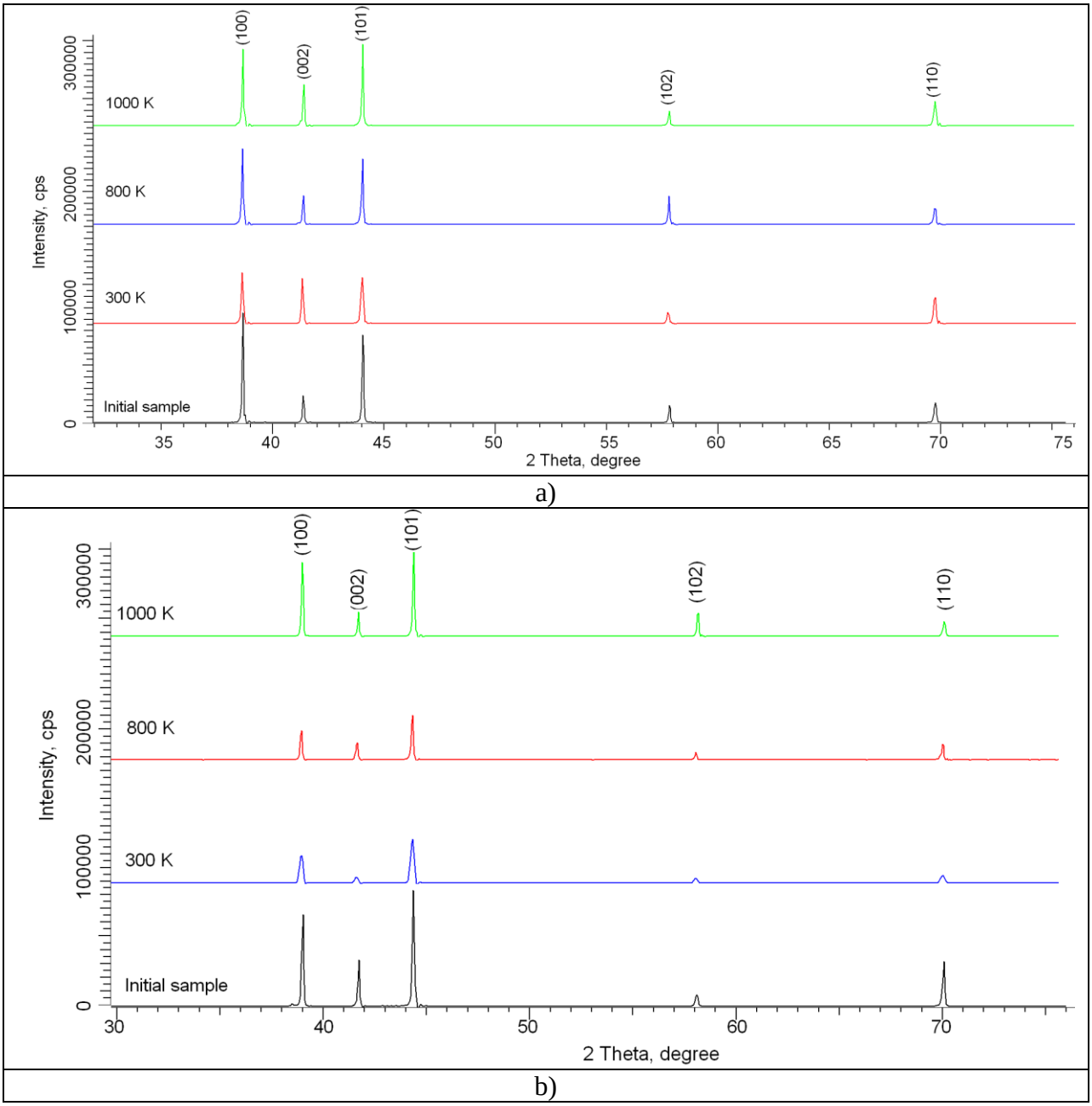

Figure 2. X-ray diffraction patterns of BeO ceramics irradiated with Ar^{8+} ions (a) and Xe^{22+} ions (b) with a fluence of $5x10^{13}$ cm^{-2} at temperatures of 300, 800, and 1000 K

Using the Rietveld method in the analysis of the shape, position and intensity of diffraction peaks, it was found that the initial samples are highly ordered polycrystalline structures with a hexagonal type of the crystal lattice of beryllium oxide (P63mc(186)) with three pronounced directions of texture orientation (100), (002) and (101). In this case, the analysis of the X-ray diffraction patterns of the samples under study before and after irradiation showed the absence of the appearance of any new diffraction reflections or stratification of diffraction maxima, which indicates the absence of phase transformations or the formation of impurity phases as a result of irradiation. The main changes in the diffraction patterns of irradiated samples are associated with a change in the shape and intensity of the diffraction maxima, as well as their angular position relative to 2θ°. The distortion of the diffraction maxima, as well as their displacement, is associated with deformation processes arising as a result of changes in the concentration of point

defects, as well as their migration in the structure as a result of irradiation. In the case of samples irradiated with Ar^{8+} ions at a temperature of 300 K, the greatest change in the intensities of the diffraction maxima, their broadening and line asymmetry are observed. A decrease in intensities indicates a reorientation of crystallites as a result of irradiation, and broadening of lines indicates grain fragmentation and recrystallization processes.

For samples irradiated with Xe^{22+} ions at a temperature of 300 K, a similar situation is observed with a change in the intensities, shape, and width of diffraction reflections, as in the case of irradiation with Ar^{8+} ions, however, the changes are more pronounced. This difference is caused not only by an increase in the depth of damage to the material upon irradiation with Xe^{22+} ions, but also by a large number of vacancy and point defects arising during irradiation. In this case, the increase in energy losses in collisions with the electronic and nuclear subsystems of the target in the case of irradiation with Xe^{22+} ions is 4 times greater and 8 times for electronic and nuclear losses, respectively, compared with similar values for irradiation with Ar^{8+} ions. This leads to an increase in the concentration of defect regions in the structure, as well as to a large number of initially knocked out atoms. Also, in the case of irradiation with Xe^{22+} ions, a sharp decrease in the intensities of the (100) and (002) reflections is observed, which indicates a strong reorientation of grains in the structure, as well as their fragmentation. However, these changes are more pronounced for irradiation with Xe^{22+} ions, which is caused not only by an increase in the depth of damage to the material, but also by a 6.5 times larger number of vacancy defects generated by irradiation with Xe^{22+} ions in comparison with irradiation with Ar^{8+} ions (according to Monte Carlo calculations in the SRIM- 2013). Also, in the case of irradiation with Xe^{22+} ions, a significant decrease in the intensities of diffraction peaks with Miller indices (100) and (002) is observed, which indicates a strong reorientation of grains in the structure, as well as their fragmentation, which is confirmed by a large broadening of reflections.

Increasing the FWHM value, i.e. physical broadening, diffraction lines provides information on the appearance of distortions and microstresses in the crystal lattice, as well as changes in interplanar distances. Figure 3a shows the results of crystal lattice distortion, in particular, the ratio of the c/a parameters, which characterizes the total deformation of the crystal lattice before and after irradiation of beryllium oxide with Ar^{8+} and Xe^{22+} ions with energies of 70 MeV and 231 MeV, respectively, at a particle fluence of 5×10^{13} cm^2 and temperatures of 300, 800 and 1000 K. Оценка структурных искажений проводилась путем измерения изменений параметров кристаллической решетки до и после облучения и сравнения их с эталонными значениями.

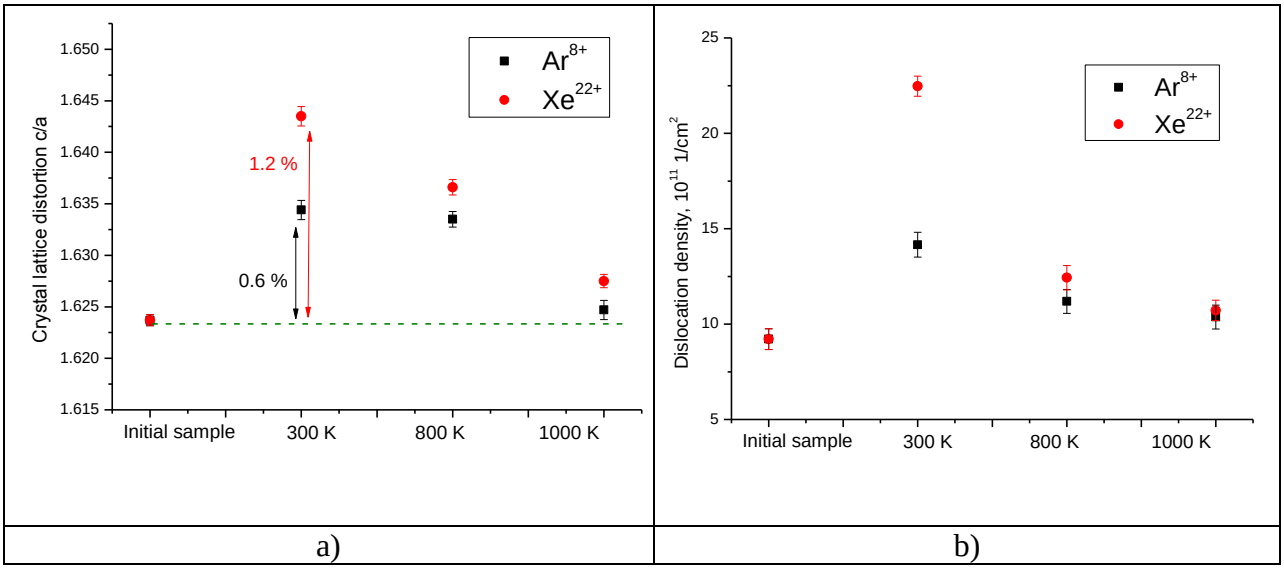

Figure 3. a) Graph of the dependence of the change in the distortion of the ratio of the crystal lattice parameters on the irradiation conditions (пунктирной линией обозначено положение

начального значения степени кристаллических искажений); b) Graph of the dependence of the change in the density of dislocations in the structure of ceramics before and after irradiation

It can be seen from the presented data that, upon irradiation with Ar^{8+} and Xe^{22+} ions at a temperature of 300 K, the degree of deformation was 0.6 % and 1.2 %, respectively. In this case, the difference in deformation by almost 2 times, depending on the type of ion, is due to energy losses and subsequent radiation damage arising from collision. However, under thermal irradiation, a decrease in the value of the crystal lattice strain is observed, and in the case of irradiation at 1000 K, this value is from 0.06 to 0.2 %, depending on the type of ion, which indicates a small deformation of the crystal lattice. Such a decrease in deformation under high-temperature irradiation is associated with a change in the magnitude of thermal vibrations of atoms in the lattice, which leads to an increase in their mobility, as well as an accelerated anighilation of arising defects in the structure.

It is well known that deformations of the crystal structure lead to an increase in the dislocation density, which significantly affects the change in both the mechanical characteristics and the optical properties of the material. Figure 3b shows the data on changes in the density of dislocations that arise during irradiation, the dynamics of which is associated primarily with the processes of crushing and recrystallization of grains. Плотность дислокаций была рассчитана на основе рентгеновских данных изменения размеров зерен в результате облучения и температурного воздействия, которые оценивались по ширине и форме дифракционных рефлексов.

As can be seen from the data presented, the main changes in the dislocation density occur at an irradiation temperature of 300 K, when the effect of annealing of defects is minimal, and the change in grain sizes is most pronounced. Moreover, in the case of irradiation at temperatures of 800 K and 1000 K, the dislocation density for both ions is practically the same (within the measurement error), and only 10-15 % exceed the values of the initial dislocation density.

As a result of elastic and inelastic collisions of incident ions with atoms of the crystal lattice, a large number of point defects and dislocations are generated, which cause an increase in microstresses and deformations of the structure. Most defects annihilate during migration, leading to relaxation of deformations and microstresses. However, at high irradiation fluences, regions of overlapping defects are formed, which form regions of nonequilibrium defect concentrations, which lead to disordering and further amorphization of the structure, which leads to a decrease in the ceramic hardness along the entire ion path, as well as to the formation of additional optical traps and an increase in the photoionization cross section, which affect on the reflectivity of BeO ceramics.

Figure 4 shows the changes in the OSL signal bleaching curve obtained for samples irradiated with different ions and at different temperatures. The general view of the curves is characterized by an asymmetric bell-shaped maximum with strong shape distortion. The dynamics of the change in the curve for irradiated samples is characterized by a decrease in the intensity of the maximum, as well as by its shift. A decrease in the intensity of the bleaching signal is associated with the presence of point defects and disordered regions in the structure of ceramics, which serve as optical traps. The shift of the maxima is due to a change in their density, both in the near-surface layer and in the distribution over depth.

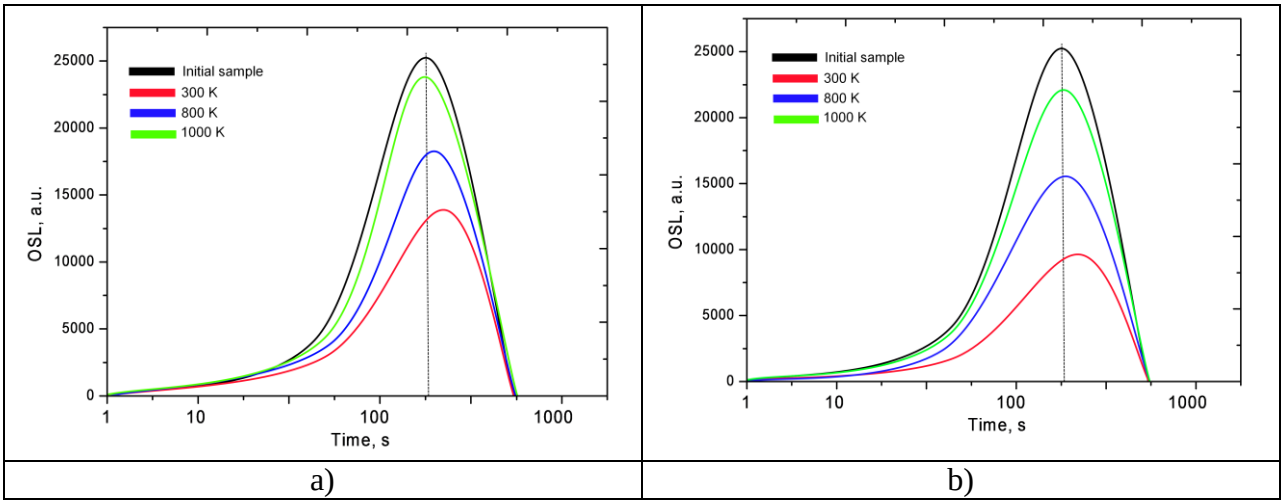

Figure 4. Dynamics of changes in OSL signal bleaching before and after irradiation with (a) Ar^{8+}; (b) Xe^{22+} ions at a radiation dose of $5x10^{13}$ ion/cm^2 and temperatures of 300, 800, and 1000 K

For the samples irradiated at different temperatures, a less pronounced decrease in the intensity of the maximum with increasing temperature is observed, which indicates a change in the concentration of optical traps with a decrease in the photoionization cross section.

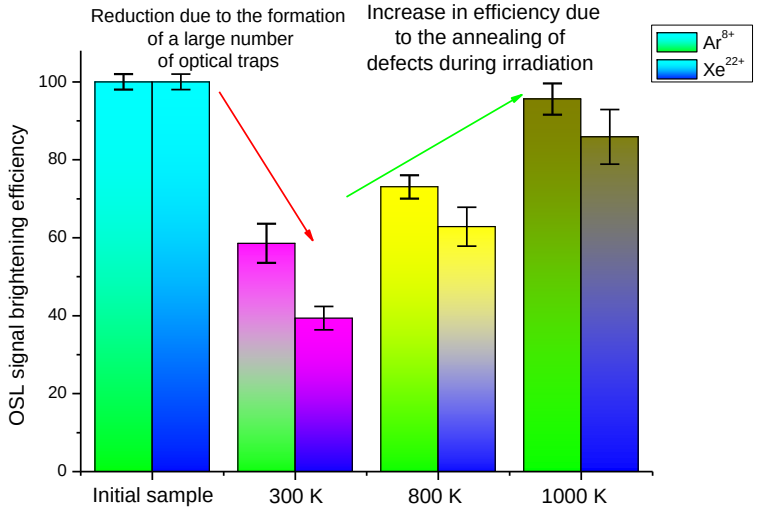

Figure 5. Diagram of the change in the efficiency of OSL signal bleaching as a result of irradiation

Figure 5 shows the OSL signal bleaching efficiency data depending on the irradiation conditions. The presented data show that in the case of irradiation at room temperature, the decrease in the bleaching efficiency is more than 40 % for the samples irradiated with Ar^{8+} ions and more than 60 % for the samples irradiated with Xe^{22+} ions. The difference in the decrease in the bleaching efficiency of 20 % is associated with a change in the density of defects arising from irradiation and the maximum ion path length, which leads to damage at a greater depth. In the case of an increase in the irradiation temperature to 800 K, a smaller decrease in the bleaching efficiency is observed, and at a temperature of 1000 K, the efficiency loss is no more than 5-15 %, depending on the type of ion. This effect is associated with the partial annealing of point defects and lower structural distortions arising during irradiation as a result of an increase in thermal vibrations of atoms in the lattice at elevated temperatures. Полученные данные также имеют хорошее согласие с данными изменения структурных искажений и плотности дислокаций, изменяющихся в результате различных режимов облучения. Как известно, на оптические

свойства большое влияние оказывает изменение концентрации точечных дефектов в структуре. При этом в случае облучения, конечным результатом радиационных повреждений является формирование областей разупорядоченности, содержащих в себе большое количество точечных дефектов и дислокаций. Наличие подобных областей приводит к изменению электронной плотности материала, а также изменению оптических свойств, как за счет изменения величины ширины запрещенной зоны, так и за счет образования дополнительных препятствий и поглощающих центров. В случае же облучения при повышенных температурах, когда часть образовавшихся дефектов в результате облучения рекомбинирует друг с другом или отжигается, степень влияния на изменение оптических характеристик существенно меньше, чем в случае облучения при комнатных температурах.

Figure 6 shows the graphs of changes in the microhardness value depending on the type of incident ion, as well as the irradiation temperature. As can be seen from the data presented, for all irradiated samples, a decrease in the value of microhardness is observed along the entire path of incident ions. In this case, an increase in the irradiation temperature leads not only to a decrease in radiation damage, but also in the depth of radiation damage. Согласно полученным данным, в случае облучения ионами Ar^{8+} максимальная глубина радиационных повреждений составляет 10-12 мкм, в то время как для облученных образцов ионами Xe^{22+} данная величина составляет более 15 мкм. Такая разница в первую очередь обусловлена различными энергетическими потерями ионов в материале в зависимости от их энергии, а также в случае облучения ионами Xe^{22+} на большей части длины пробега доминируют неупругие столкновения ионов с электронной подсистемой, что зарождает в структуре керамик большое количество первично выбитых электронов, способных создавать каскады вторичных электронов. В этом случае, облучение приводит к образованию большого количества локализованных дефектных областей, приводящих к возникновению деформационных искажений кристаллической структуры, а также частичному разрушению кристаллических и химических связей, что и приводит к снижению прочностных свойств. Однако, в случае облучения при повышенных температурах, процесс формирования радиационных дефектов конкурирует с их рекомбинацией и температурным отжигом дефектов. При этом увеличение температуры облучения приводит к тому, что большая часть образованных радиационных точечных дефектов аннигилирует за счет нагрева. Результатом чего наблюдается меньшее искажение структуры и, следовательно, меньшее изменение механических и прочностных свойств.

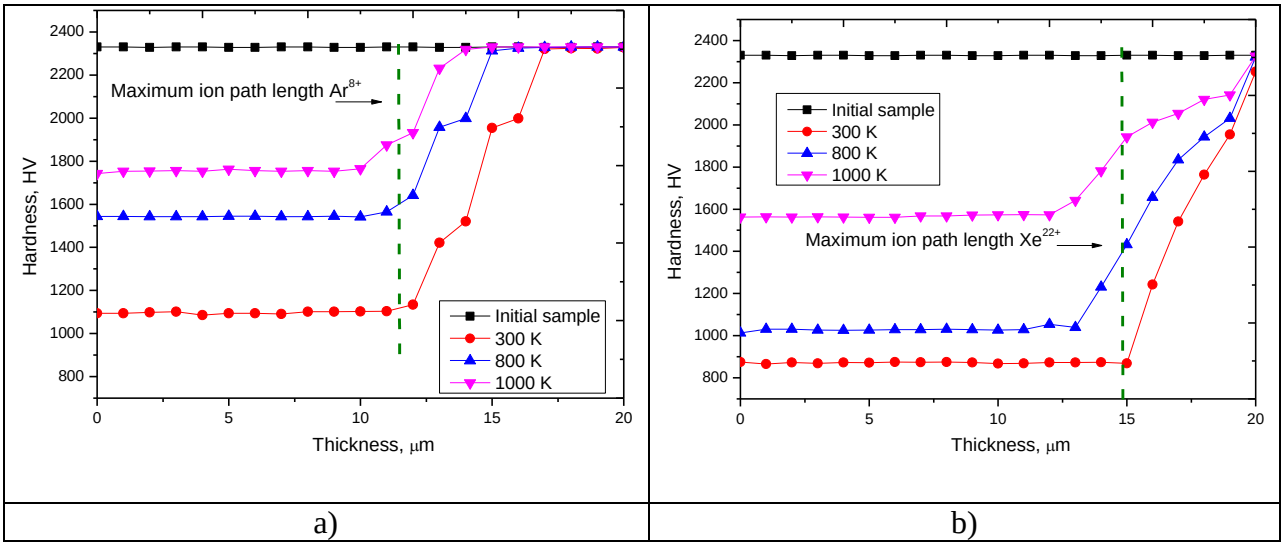

Figure 6. A graph of the dependence of the change in the microhardness of BeO ceramics depending on the type of irradiation: a) Ar^{8+}; b) Xe^{22+}

On the basis of the obtained data on changes in microhardness, the efficiency of microhardness resistance to radiation damage resulting from irradiation with various ions and irradiation temperature was calculated. The calculation data are presented in Figure 7. According to the data obtained, in the case of irradiation of ceramics at a temperature of 300 K, a sharp decrease in microhardness by 50-60% is observed, depending on the type of irradiation. In this case, an increase in the irradiation temperature leads to a decrease in the degree of radiation damage.

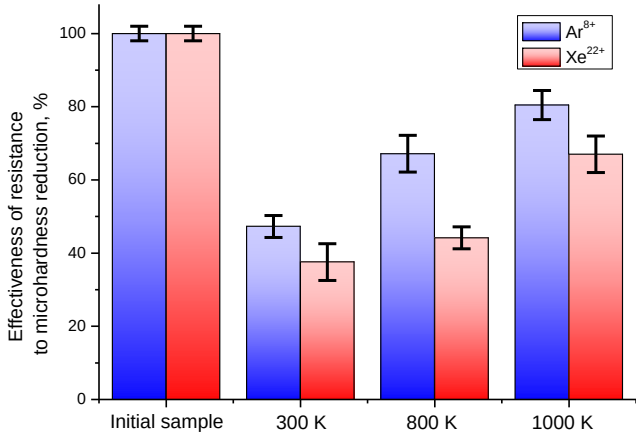

Figure 7. Diagram of the effectiveness of microhardness resistance to radiation damage

The general trend in the change in the surface morphology of irradiated ceramics is associated with a change in the surface relief as a result of defect formation, deformation of the crystal structure, and partial sputtering of the near-surface layer. Figure 8 shows 3D images of the surface morphology of BeO ceramics before and after irradiation, performed using the method of atomic force microscopy.

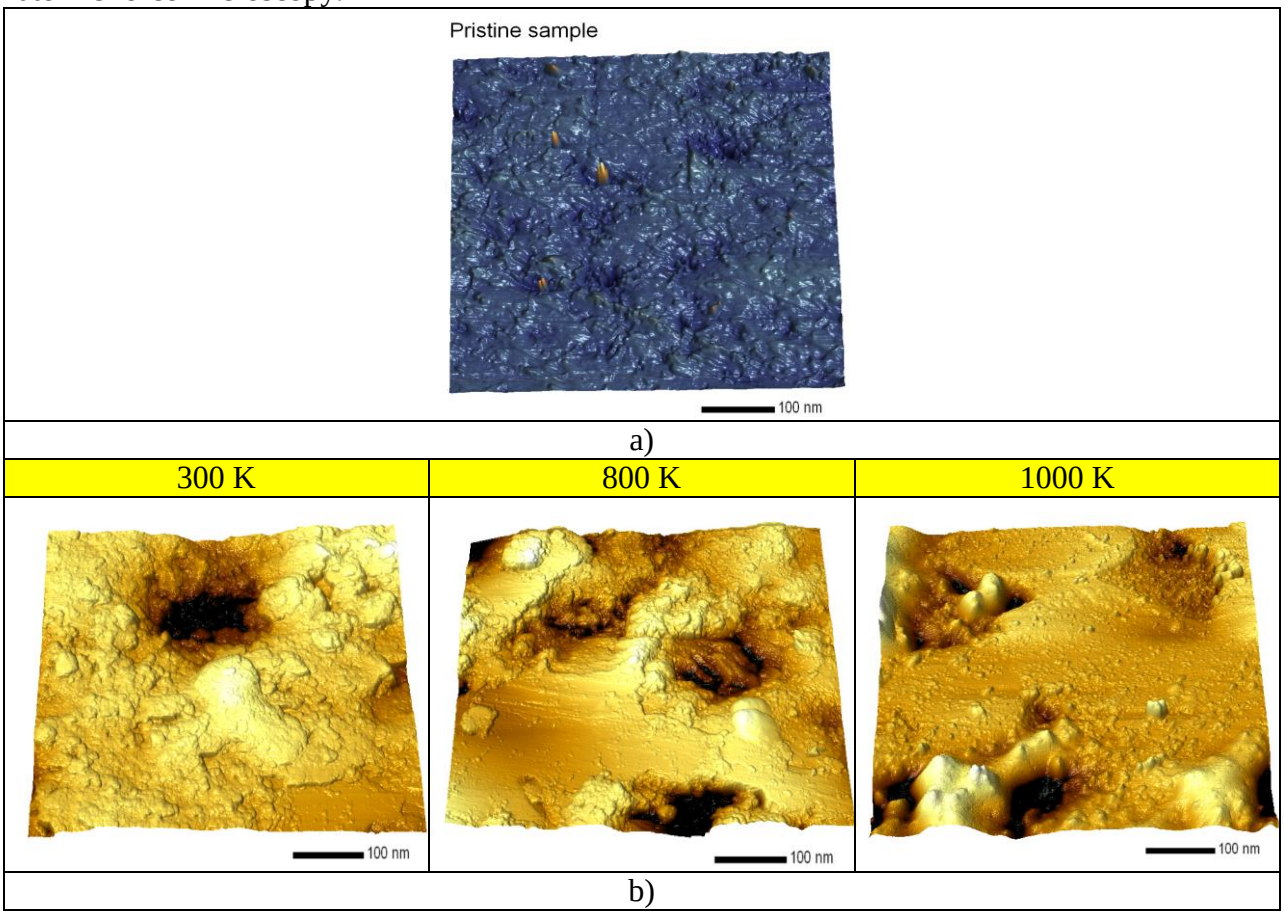

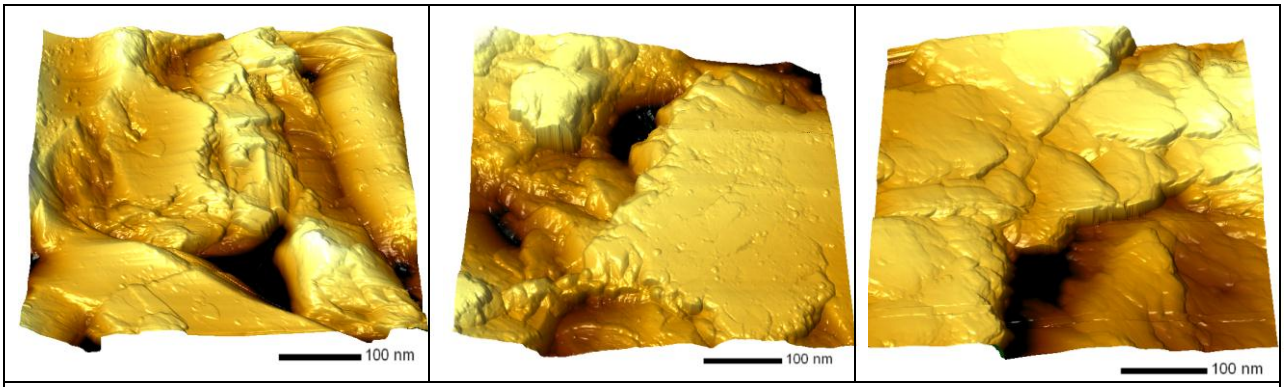

c)

Figure 8. Data on changes in the surface morphology of the investigated ceramics before irradiation (a) and after irradiation with (b) Ar^{8+} ions; c) Xe^{22+}

The general tendency of changes in the surface morphology of irradiated ceramics is associated with a change in the surface relief as a result of defect formation, deformation of the crystal structure, and partial sputtering of the surface layer. For samples irradiated with Ar^{8+} ions, the main effects of changes in the surface topography are associated with the formation of crater formations, which are formed as a result of partial peeling of the surface layer as a result of the appearance of overvoltage regions and highly disordered regions. For example, on the surface of ceramics, the formation of hillock-like inclusions is observed, resulting from the extrusion of a deformed volume onto the surface as a result of radiation damage. In this case, an increase in the irradiation temperature leads to a decrease in the density of these inclusions, as well as to a decrease in their size, which indicates the effect of partial annealing of defects at high irradiation temperatures. For samples irradiated with Xe^{22+} ions, the main changes in the surface relief are associated with partial exfoliation and crater formation as a result of irradiation. In this case, the tendency for a decrease in the change in the surface relief with an increase in the irradiation temperature is similar, as for the samples irradiated with Ar^{8+} ions.
Thus, during this study, it was found that thermal irradiation leads to a decrease in the degree of radiation damage and a decrease in their contribution to structural changes. It has been shown that BeO ceramics exposed to high-temperature irradiation are more resistant to degradation and deformation of their structural and strength properties.

Conclusion

The paper presents study results on high-temperature irradiation of BeO ceramics with swift heavy ions. Distortion of diffraction peaks and their shift are associated with deformation processes arising from changes in concentration of point defects, as well as their migration in the structure as a result of irradiation. Irradiation of BeO ceramics with Ar^{8+} and Xe^{22+} ions at a temperature of 1000 K leads to comparable for given particles changes in dislocation density, optically stimulated luminescence intensity and microhardness. The results obtained indicate the process of defect annealing and microstress relaxation of the crystal lattice, which arise during irradiation as a result of increase in thermal vibrations of atoms in the lattice at elevated temperatures. Thus, it has been established that high-temperature irradiation of BeO ceramics reduces effect of electron and nuclear energy losses of Ar^{8+} and Xe^{22+} ions with energies of 70 MeV and 231 MeV, respectively, on defect formation efficiency. This is associated with an increase in magnitude of thermal vibrations of lattice atoms, leading to an increase in their mobility, as well as accelerated annihilation of generated defects with partial recovery of the optical properties and hardness of the ceramics.
In conclusion, the data obtained on the effect of high-temperature irradiation of beryllium oxide on the decrease in the contribution of the electronic and nuclear energy losses of high-energy

heavy ions to the degree of radiation damage make it possible to determine the thermal stability and the range of applicability of BeO ceramics in high-temperature fields.

Funding
This research was funded by the Science Committee of the Ministry of Education and Science of the Republic of Kazakhstan (No. AP08855828).

References

1. Prakash, Deo, et al. "Synthesis, purification and microstructural characterization of nickel doped carbon nanotubes for spintronic applications." Ceramics International 42.5 (2016): 5600-5606.
2. Souadia, Z., et al. "Electronic structure and optical properties of the dialkali metal monotelluride compounds: Ab initio study." Journal of Molecular Graphics and Modelling 90 (2019): 77-86.
3. Rais, A., et al. "Copper substitution effect on the structural properties of nickel ferrites." Ceramics International 40.9 (2014): 14413-14419.
4. Al-Gaashani, R., et al. "XPS and optical studies of different morphologies of ZnO nanostructures prepared by microwave methods." Ceramics International 39.3 (2013): 2283-2292.
5. Ghaffour, M., et al. "Study by aes and eels of InP, InSb, InPO4 AND In x Ga 1-x As submitted to electron irradiation." Surface Review and Letters 19.01 (2012): 1250002.
6.Alnujaim, S., et al. "Ab initio prediction of the elastic, electronic and optical properties of a new family of diamond-like semiconductors, Li2HgMS4 (M= Si, Ge and Sn)." Journal of Alloys and Compounds 843 (2020): 155991.
7. Salik, L., et al. "Structural, elastic, electronic, magnetic, optical, and thermoelectric properties of the diamond-like quaternary semiconductor CuMn 2 InSe 4." Journal of Superconductivity and Novel Magnetism 33.4 (2020): 1091-1102.
8. Hadji, S., et al. "Elastic, electronic, optical and thermodynamic properties of Ba3Ca2Si2N6 semiconductor: First-principles predictions." Physica B: Condensed Matter 589 (2020): 412213.
9. Bouchenafa, M., et al. "Theoretical investigation of the structural, elastic, electronic, and optical properties of the ternary tetragonal tellurides KBTe2 (B= Al, In)." Materials Science in Semiconductor Processing 114 (2020): 105085.
10. Touam, S., et al. "First-principles computations of YxGa1-x As-ternary alloys: a study on structural, electronic, optical and elastic properties." Bulletin of Materials Science 43.1 (2020): 1-11.
11. Benali, M. A., et al. "Synthesis and analysis of SnO2/ZnO nanocomposites: Structural studies and optical investigations with Maxwell–Garnett model." Materials Chemistry and Physics 240 (2020): 122254.
12. Al-Douri, Y., et al. "First-Principles Calculations to Investigate the Refractive Index and Optical Dielectric Constant of Na3SbX4 (X= S, Se) Ternary Chalcogenides." physica status solidi (b) 256.11 (2019): 1900131.
13. Al-Douri, Y., Ali Abu Odeh, and A. S. Ibraheam. "Transition metals doped In2S3 nanostructure: structural and optical features." Materials Research Express 6.12 (2020): 125914.
14. Sagadevan, Suresh, et al. "Synthesis and evaluation of the structural, optical, and antibacterial properties of copper oxide nanoparticles." Applied Physics A 125.8 (2019): 1-9.
15. Al-Douri, Yarub, Noureddine Amrane, and Mohd Rafie Johan. "Annealing temperature effect on structural and optical investigations of Fe2O3 nanostructure." Journal of Materials Research and Technology 8.2 (2019): 2164-2169.
16. Badi, Nacer, Yarub Al-Douri, and Syed Khasim. "Effect of nitrogen doping on structural and optical properties of MgxZn1-xO ternary alloys." Optical Materials 89 (2019): 554-558.

17. Dulera, I. V., and R. K. Sinha. "High temperature reactors." Journal of Nuclear Materials 383.1-2 (2008): 183-188.
18. Li, D. S., H. Garmestani, and Justin Schwartz. "Modeling thermal conductivity in UO2 with BeO additions as a function of microstructure." Journal of Nuclear Materials 392.1 (2009): 22-27.
19. Nanto, Hidehito. "Photostimulable storage phosphor materials and their application to radiation monitoring." Sensors and Materials 30.3 (2018): 327-337.
20. Kadyrzhanov, K. K., K. Tinishbaeva, and V. V. Uglov. "Investigation of the effect of exposure to heavy Xe22+ ions on the mechanical properties of carbide ceramics." Eurasian Phys. Tech. J 17 (2020): 46-53.
21. Zhang, J., et al. "Light He and heavy Kr ions irradiation effects in orthorhombic Tb2TiO5 ceramics." Nuclear Instruments and Methods in Physics Research Section B: Beam Interactions with Materials and Atoms 441 (2019): 88-92.
22. Carniglia, S. C., et al. "Hot pressing for nuclear applications of BeO; process, product, and properties." Journal of Nuclear Materials 14 (1964): 378-394.
23. Camarano, D. M., et al. "Thermal Conductivity of UO 2–BeO–Gd 2 O 3 Nuclear Fuel Pellets." International Journal of Thermophysics 40.12 (2019): 110.
24. Santos, Alexandre M. Caraça, Mohammad Mohammadi, and Shahraam Afshar. "Investigation of a fibre-coupled beryllium oxide (BeO) ceramic luminescence dosimetry system." Radiation measurements 70 (2014): 52-58.
26. Jahn, A., et al. "The BeOmax system–Dosimetry using OSL of BeO for several applications." Radiation measurements 56 (2013): 324-327.
27. Kislitsin, S. B., et al. "Degradation processes and helium swelling in beryllium oxide." Surface and Coatings Technology 386 (2020): 125498.
28. Altunal, V., et al. "Investigation of luminescence properties of BeO ceramics doped with metals for medical dosimetry." Optical Materials 108 (2020): 110436.
29. Yasuda, H., and K. Fujitaka. "Glow curves from beryllium oxide exposed to high energy heavy ions." Radiation protection dosimetry 87.3 (2000): 203-206.
30. Bulur, Enver. "More on the TR-OSL signal from BeO ceramics." Radiation measurements 66 (2014): 12-20.
31. Teichmann, T., et al. "Dose and dose rate measurements in proton beams using the luminescence of beryllium oxide." Journal of Instrumentation 13.10 (2018): P10015.
32. David, L., et al. "Characterization of thermal conductivity degradation induced by heavy ion irradiation in ceramic materials." Journal of Physics D: Applied Physics 41.3 (2008): 035502.
33. Lian, J., et al. "Heavy ion irradiation effects of brannerite-type ceramics." Nuclear Instruments and Methods in Physics Research Section B: Beam Interactions with Materials and Atoms 191.1-4 (2002): 565-570.
34. Mirzayev, Matlab N., et al. "Thermophysical behavior of boron nitride and boron trioxide ceramics compounds with high energy electron fluence and swift heavy ion irradiated." Journal of Alloys and Compounds (2020): 155119.
35. Liu, Kui, et al. "Heavy-ion irradiation effects of Gd2Zr2O7 nanocrystalline ceramics as nuclear waste immobilization matrix." Journal of Nuclear Materials (2020): 152236.
36. Florez, Raul, et al. "The irradiation response of ZrC ceramics under 10 MeV Au3+ ion irradiation at 800 ºC." Journal of the European Ceramic Society 40.5 (2020): 1791-1800.
37. Lawson, Sebastian M., et al. "Synthesis and in situ ion irradiation of A-site deficient zirconate perovskite ceramics." Journal of Materials Chemistry A 8.37 (2020): 19454-19466.
38. Qarra, Hassan H., et al. "Heavy ion irradiation damage in Zr3 (Al0. 9Si0. 1) C2 MAX phase." Journal of Nuclear Materials 540 (2020): 152360.
39. Bowden, D., et al. "The stability of irradiation-induced defects in Zr3AlC2, Nb4AlC3 and (Zr0. 5, Ti0. 5) 3AlC2 MAX phase-based ceramics." Acta Materialia 183 (2020): 24-35.

40. Trukhanov, A. V., et al. "Control of structural parameters and thermal conductivity of BeO ceramics using heavy ion irradiation and post-radiation annealing." Ceramics International 45.12 (2019): 15412-15416.
41. Ryskulov, A. E., et al. "The effect of Ni12+ heavy ion irradiation on the optical and structural properties of BeO ceramics." Ceramics International 46.4 (2020): 4065-4070.
42. Klein, Dominic, Eugen Eisfeld, and Johannes Roth. "Molecular dynamics simulations of the laser ablation of silicon with the thermal spike model." Journal of Physics D: Applied Physics 54.1 (2020): 015103.
43. Mocanu, Felix C., Konstantinos Konstantinou, and Stephen R. Elliott. "Nonequilibrium ab initio molecular-dynamics simulations of lattice thermal conductivity in irradiated glassy Ge 2 Sb 2 Te 5." Applied Physics Letters 116.3 (2020): 031902.
44. van Vuuren, Arno Janse, et al. "Analysis of the microstructural evolution of silicon nitride irradiated with swift Xe ions." Ceramics International 46.6 (2020): 7155-7160.
45. Kamarou, A., et al. "Swift heavy ion irradiation of InP: thermal spike modeling of track formation." Physical Review B 73.18 (2006): 184107.
46. Szenes, G. "Information provided by a thermal spike analysis on the microscopic processes of track formation." Nuclear Instruments and Methods in Physics Research Section B: Beam Interactions with Materials and Atoms 191.1-4 (2002): 54-58.
47. Sall, M., et al. "Track formation in III-N semiconductors irradiated by swift heavy ions and fullerene and re-evaluation of the inelastic thermal spike model." Journal of Materials Science 50.15 (2015): 5214-5227.
48. Murty, K. L., and I. Charit. "Structural materials for Gen-IV nuclear reactors: Challenges and opportunities." Journal of Nuclear Materials 383.1-2 (2008): 189-195.
49. Fazio, Concetta, et al. "Innovative materials for Gen IV systems and transmutation facilities: The cross-cutting research project GETMAT." Nuclear Engineering and Design 241.9 (2011): 3514-3520.
50. Malerba, Lorenzo, et al. "Advances on GenIV structural and fuel materials and cross-cutting activities between fission and fusion." EPJ N-Nuclear Sciences & Technologies 6 (2020): 32.
51. Bertrand, F., et al. "Simplified criteria for a comparison of the accidental behaviour of Gen IV nuclear reactors and of PWRS." Nuclear Engineering and Design (2020): 110962.
52. Mikityuk, Konstantin, et al. "Review of Euratom projects on design, safety assessment, R&D and licensing for ESNII/Gen-IV fast neutron systems." EPJ Nuclear Sciences & Technologies 6 (2020): 36.